SEISMIC ATTRIBUTES IN IMAGING CHALLENGING RESERVOIRS: A CASE STUDY OF BOONSVILLE FIELD, NORTH CENTRAL TEXAS

MOHAMMED FARFOUR and WANG JUNG YOON

Chonnam National University, Dept. of Energy and Resources Engineering, Geophysical Prospecting Laboratory, 300 Yongbong-Dong, Buk-gu, Gwangju, 500-757, South Korea. wjyoon@chonnam.ac.kr

(Received September 16, 2014; revised version accepted February 25, 2015)

ABSTRACT

Farfour, M. and Yoon, W.J., 2015. Seismic attributes in imaging challenging reservoirs: a case study of Boonsville Field, North Central Texas. *Journal of Seismic Exploration*, 24: 169-185.

In this study, we investigate the Caddo sequence from the Boonsville gas field in the Fort Worth Basin of North Central Texas. Two Middle Pennsylvanian thin reservoirs are closely separated by a thin Caddo limestone unit. Seismic attributes, namely, instantaneous frequency and amplitude attributes did predict the distribution of reservoir facies in some productive wells. Also, the attribute maps implied that the Caddo facies would exist at well locations where the reservoir was not encountered and were absent where their presence was confirmed from well control. To remove this ambiguity, more advanced techniques of filtering, tracking and information extraction have been invoked and integrated. The data were firstly subject to dip-steered filtering and dense tracking processes. Next, the cleaned data set was spectrally decomposed using a Time Frequency Continuous Wavelet Transform. This decomposition successfully resolved both reservoirs. However, some non-reservoir areas were characterized by frequency responses similar to those shown in reservoir areas. Spectral examination of individual traces from producing and non-producing areas inferred that producing zones are characterized by frequency features different than those of the nonproducing zones. Next, poststack seismic inversion was performed to incorporate well data with seismic data and to produce an acoustic impedance cube. Interestingly, the acoustic impedance sections also suggested that the productive sandstones are characterized by different and higher impedance character relative to limestone formations and their surroundings.

This study demonstrates that incorporating information from different sources (amplitude, frequency, spectral decomposition, well data, etc.) can assist significantly in overcoming challenging formations in the subsurface.

KEY WORDS: Continuous Wavelet Transform, spectral decomposition, acoustic impedance, thin reservoir.

0963-0651/15/$5.00

INTRODUCTION

Seismic attributes are defined as all of the measured, computed, or implied quantities that can be obtained from the seismic data. This list includes complex trace attributes (e.g. instantaneous amplitude, frequency, phase, etc.), seismic event geometrical configurations (dip, azimuth, curvature, coherency, etc.), and their spatial and pre-stack variations. Attributes are related to the fundamental information in seismic data: time, amplitude, frequency, and attenuation. Time-derived attributes help to discern structural detail. Amplitude-derived and frequency-derived attributes address problems of stratigraphy and reservoir properties. Spectral decomposition is an example of innovative seismic attributes that are widely used for reservoir imaging and interpretation technology, originally developed and commercialized by BP, Apache Corporation and Landmark (Partyka et al., 1999). This technology decomposes a seismic broad band spectrum into its constituent frequency components to yield much higher resolution images of reservoir boundaries, lithologic heterogeneities, and interval thicknesses than do traditional full-band seismic displays (Burns and Street, 2005). In fact, over the last decade numerous published works discussed how this new attribute can be used to differentiate both lateral and vertical lithologies and pore fluid changes. The attribute has been successfully used, as well, in delineating stratigraphic traps and identifying subtle frequency variations caused by hydrocarbons (see for example Castagna et al., 2003; Castagna and Sun, 2006; Farfour et al., 2013; Yoon and Farfour, 2012,).

In a previous study by Hardage et al. (1996a), seismic instantaneous attributes have been used to define the Upper and Lower Caddo reservoir facies distribution. They treated each reservoir with a different attribute. They used instantaneous frequency to map the Lower Caddo and averaged instantaneous amplitude for Upper Caddo imaging. The attributes could indicate some parts of the Lower Caddo but failed to map the Upper Caddo. Thus, more advanced attributes were suggested and more thorough analysis was recommended by the authors to overcome this problem. Later on, Tanakov and Kelkar (2000) and Xie et al. (2004) have integrated well data and used different approaches to map the Caddo reservoir. While the first study used geo-statistical methods (krigging, co-krigging) to predict reservoir properties, the second has employed cross-correlation of selected reference traces at well locations to identify different facies of the Caddo formation.

In this study, the strategy that addresses the reservoir is different. After some modern poststack filtering processes, a very dense and careful mapping technique was invoked to track the target horizon. We then used a Time Frequency Continuous Wavelet Transform to study the spectral-decomposition response to stratigraphic features of the Caddo sequence of Middle Pennsylvanian age. The decomposition successfully resolved both reservoir

distributions and delivered facies extensions that correlated very well with well data. However, some similar frequency responses to that of the Lower Caddo have been observed at non-productive zones. Traces from the two different zones have been extracted and subjected to more detailed spectral analysis. The frequency response of the productive zone was found to be different from the nonproducing one. Additionally, a cropped seismic cube spanning the zones under investigation has been inverted for acoustic impedance. The acoustic impedance images could support findings from the spectral image interpretation and also discriminate the two formations from each other.

GEOLOGICAL SETTING

The Boonsville gas field is located in the Fort Worth Basin of North-Central Texas (Fig. 1). The reservoir system we study is the Bend Conglomerate, a productive series of gas reservoirs composed of Middle Pennsylvanian fluvio-deltaic clastics about 900 to 1300 ft (275 to 400 m) thick in our project area, with the base of the interval being a little less than 5000 ft (1525 m) deep (Fig. 2).

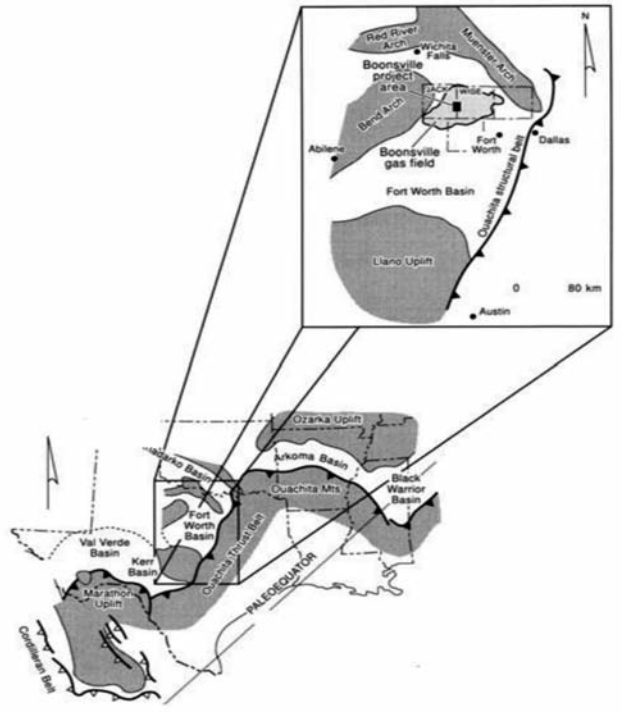

Fig. 1. Boonsville project area. The solid rectangle on the Wise-Jack county line designates the area where 3D seismic data were gathered and where most of the research work was performed (From Hardage et al., 1996a).

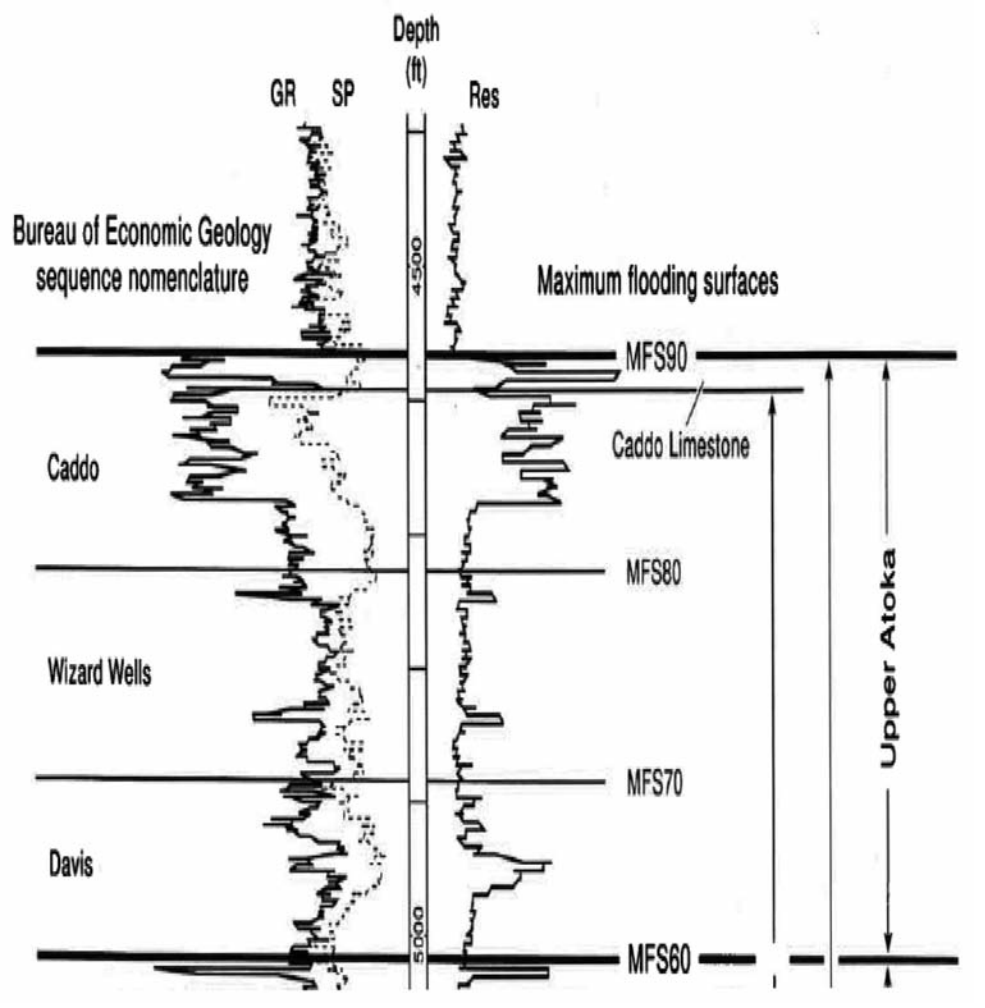

Fig. 2. Bend conglomerate genetic sequence in Boonsville field (From Hardage et al., 1996b).

We focus particularly on the Caddo interval which is one of the most productive reservoirs in the area. The Caddo sequence contains two discrete sandstone bodies, one within the Lower Caddo between Maximum Flooding surface (MFS80) and the Caddo limestone and one in the Upper Caddo between Maximum Flooding surface MFS90 and the Caddo limestone (Fig. 2).

Note that most of the Caddo production in our study area is oil; however, significant gas reserves have been found in some Upper Caddo wells that are located structurally downdip relative to the Lower Caddo oil accumulations. This finding indicates that the two units are physically separate reservoir compartments.

METHODOLOGY

Our primary seismic imaging objective is to delineate the Lower and Upper Caddo reservoirs boundaries and to distinguish sand-fill from limestone-fill distributions. A very dense auto tracking approach was invoked to avoid tracking uncertainties and errors. First, a dip "steering cube" is generated which calculates local dip and azimuth at every sample position within the seismic volume. The smoothed steering cube is subsequently used to run poststack filtering to improve the data interpretability and resolution. Then, with the help of the steering cube we generate a set of auto-tracked horizons that are typically separated by one time sample point (De Grout et al., 2010). Indeed, this advanced mapping technique enabled us to track our horizons rapidly and confidently. Note that both reservoirs here are within a data window that spans 30 ms. After that, we run spectral decomposition using continuous wavelet transform (CWT). In practice, the CWT approach involves the following steps:

- Decompose the seismogram into wavelet components.
- Multiply the complex spectrum of each wavelet used in the basis function by its CWT coefficient and sum the result to generate instantaneous frequency gathers.
- These gathers then sorted to produce constant frequency cubes, time slices, horizon slices, or vertical sections (Chopra and Marfurt, 2007).

In our case, a Mexican Hat wavelet (Mallat, 2008) was selected among other available wavelets. Then, CWT images are calculated by setting the attribute at an initial frequency component which will change (increase or decrease) by predefined increments.

After that, we study the spectral-decomposition responses relevant to different lithology fills at different frequencies. Each frequency component is expected to enable the interpretation of subtle details of the stratigraphic framework of the reservoir. Some frequency responses similar to that of the Lower Caddo reservoir have been observed at non-productive zones. Traces from the two different zones have been extracted and subjected to more detailed spectral analysis. Then, a cropped seismic volume covering the zone of interest was inverted for acoustic impedance. For that purpose, seismic horizons and well logs are used to build an initial model. The model is then updated iteratively and then convolved with a seismic wavelet extracted from the data to create a synthetic volume. This synthetic volume is continuously compared with real data until a maximum fit is reached and error approaches minimum values (Hampson et al., 2005).

RESULTS AND DISCUSSION

Examination of the Boonsville 3D seismic data showed that the seismic reflection associated with the Caddo sequence boundary underwent a significant amplitude reduction along the trend where the well-log-based map showed that the Upper Caddo reservoir sandstone existed. Thus, seismic reflection amplitude was not unambiguous tool for characterizing this challenging reservoir. In fact, it has been noted that the Caddo reflection event develops a doublet character when productive facies are present. However, these doublet reflections were found to be a misleading character in the northwest area of the field. In Figs. 3 and 4 two seismic sections passing by two different wells, one well is dry and the other is producing well. Note how the seismic characters at producing and dry wells (I.G.Y13 and B.Y.18D respectively.) look similar although the productive Caddo facies was not penetrated at the well B.Y18D.

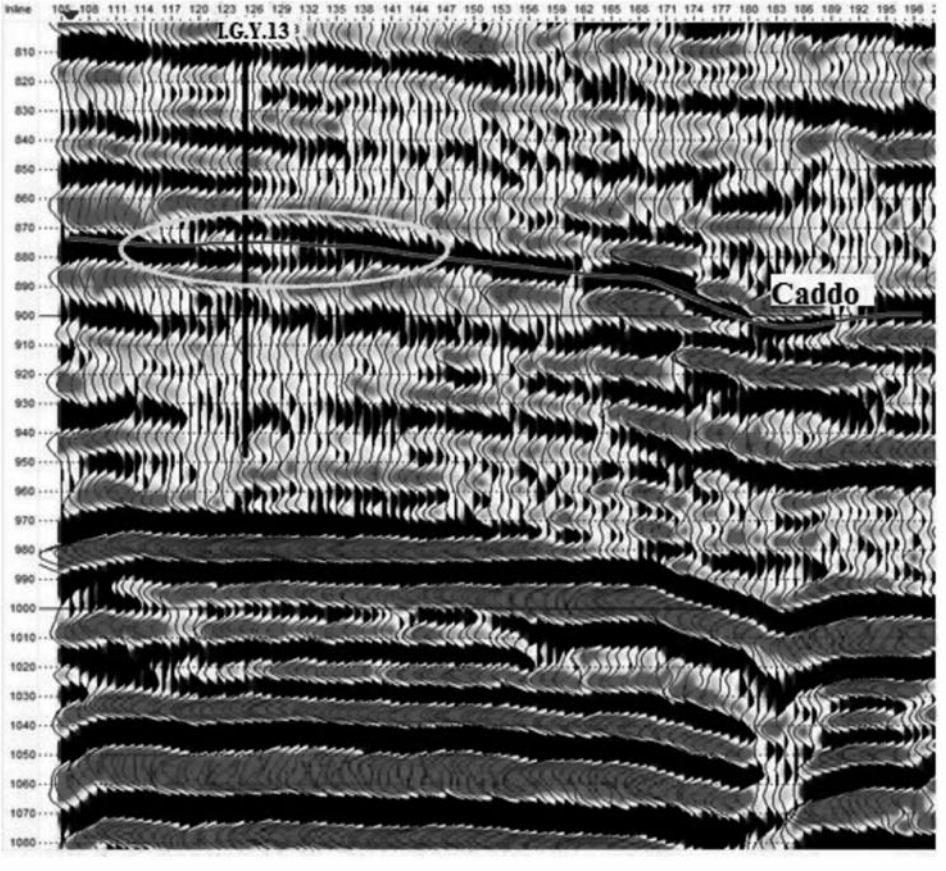

Fig. 3. A seismic crossline traversing a producing well (I.Y.13). Note the doublet character that the Caddo develops at the productive facies.

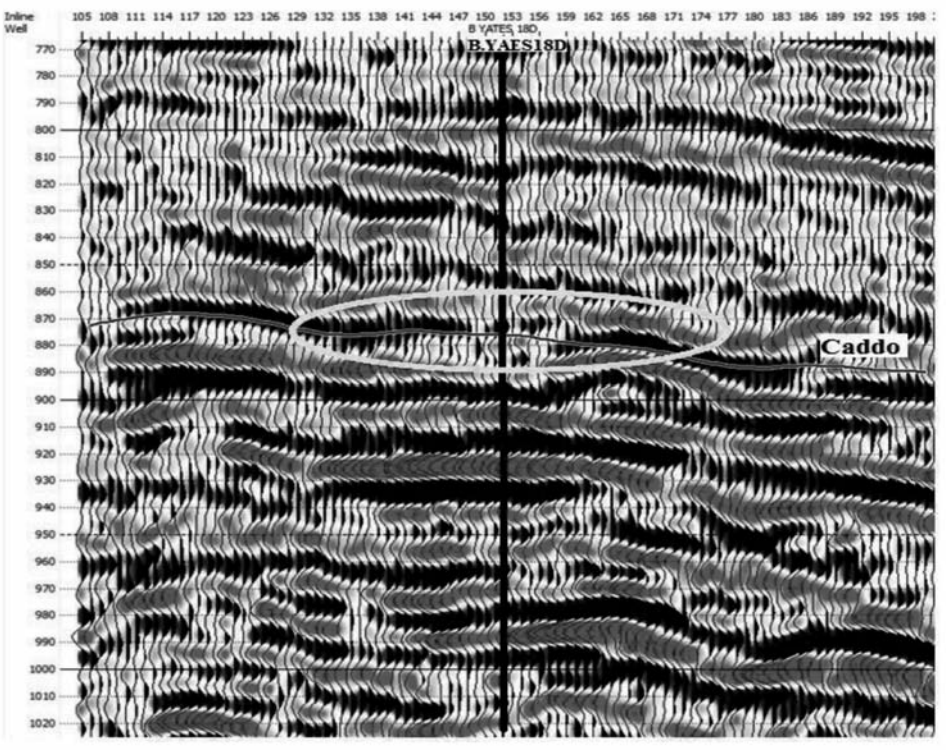

Fig. 4. A seismic crossline traversing the B.Y.18D well. Note that this dry well penetrates two thin non-productive limestone units.

Results from a previous study by Hardage et al. (1996a) showed that some areas of the Lower Caddo reservoir can be observed using seismic attributes (Figs. 5 and 6). While the averaged instantaneous frequency map in Fig. 5 did predict some parts of the Lower Caddo and show results that are somewhat consistent with well based maps, averaged instantaneous amplitude in Fig. 6 failed to predict the Upper Caddo reservoir facies distribution unambiguously. Indeed, the latter attributes indicates the limestone beds as productive sandstone.

We then have anticipated that incorporating more advanced techniques may help solve this problem. Dip-steered filtering processes were applied to the data to improve reflection continuity, resolution, and interpretability. Subsequently, a wavelet-based spectral decomposition was applied to the data.

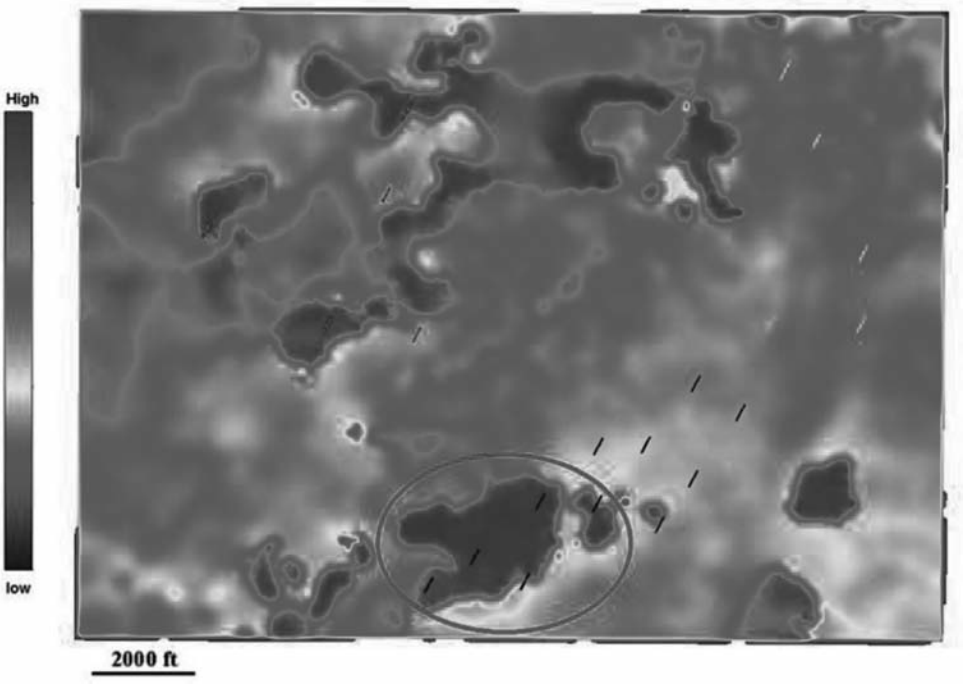

Fig. 5. Average instantaneous seismic frequency calculated within the Lower Caddo sequence. This map is found correlates with the Lower Caddo net reservoir sandstone map. Wells in black produce from The Lower Caddo, while wells in yellow produce from the Upper Caddo. Higher frequencies in the Lower Caddo zone coincide with net reservoir (circle).

For this decomposition a Mexican hat wavelet was found to be the best choice in terms of lateral frequency and vertical time resolutions. In Fig. 6, displayed are the different wavelets used for the spectral analysis.

Fig. 8 shows how clearly the Mexican hat wavelet decomposes the seismic trace into sub-frequencies compared to Gaussian and Morlet wavelets (Mallat, 2008). Several frequencies have been calculated for the carefully tracked Caddo horizon. At 50 Hz the reservoir horizon frequency amplitude showed a similar trend to that was observed in instantaneous frequency map by Hardage et al. (1996a), and an important correlation was observed with engineering data.

Referring to Fig. 9, the 50-Hz frequency image, surprisingly, could map not only the Lower Caddo but also the Upper Caddo as it is shown in the northeastern part of the image space. Notice that both reservoirs appear with

distinct character. Thus, it can be readily seen that the producing wells are penetrating different zones. AC1, AC2, AC3, AB3 and C.B21.1 (in black) are producing from one zone (Upper Caddo), whereas I.G.Y3, I.G.Y31, I.G.Y13, I.G.Y21, I.G.Y19, L.O.F1, L.O.F2, L.O.F3 and L.O.F.5 (white) are producing from another productive zone (Lower Caddo). The reason that the two reservoirs were apparent on the same horizon frequency image is due to the fact that the reservoirs are thin (below tuning) and so close vertically that their images can be seen in one horizon. Both reservoir intervals are present within a time window not exceeding 30-ms; in such situations, geologic features, or at least most features, can be seen on more than one closely spaced horizon. It is up to the interpreter to choose the interval where the feature analyzed is best resolved (Roksandic, 1995).

Furthermore, we remarkably noticed that all producing wells from Lower Caddo reservoir were found characterized by low-frequency amplitudes trending northeastward; while wells producing from Upper Caddo were found to be associated with high spectral amplitudes.

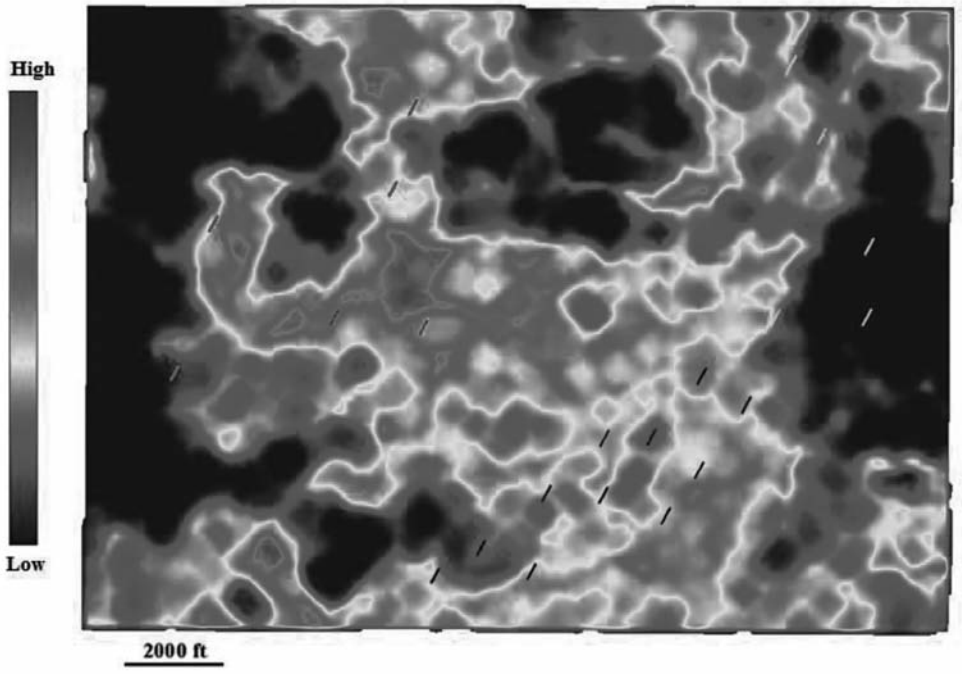

Fig. 6. Map of seismic amplitude attribute calculated within the Upper Caddo sequence. Note that wells drilled in northwestern zones were interpreted as productive. Well data implied that most of these zones are non-producing limestone zones. Wells in black produce from the Lower Caddo while wells in white produce from Upper Caddo.

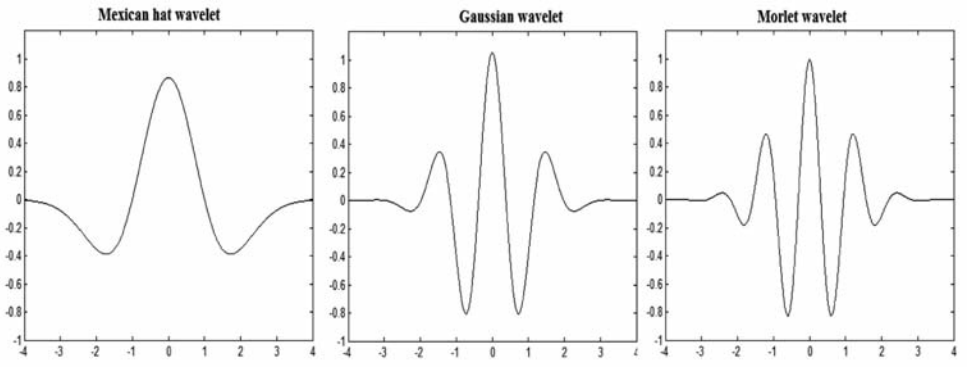

Fig. 7. The wavelets used for the spectral decomposing analysis: Mexican hat wavelet (left), Gaussian (middle) and Morlet wavelet (right).

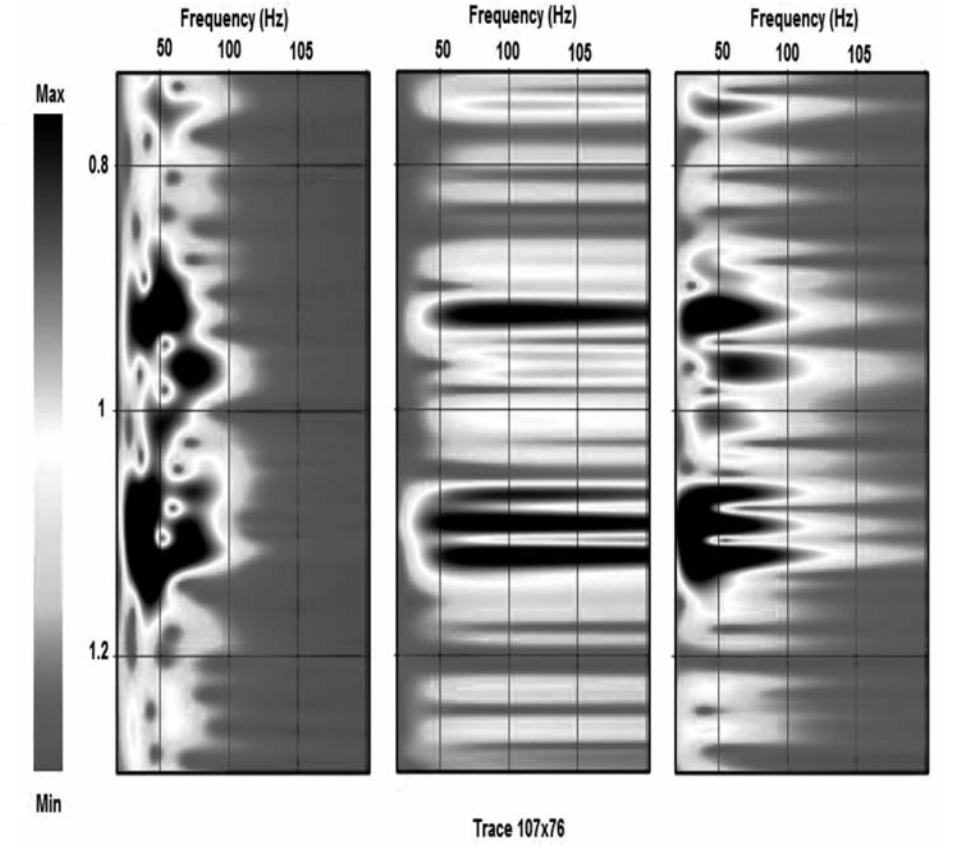

Fig. 8. Spectrally decomposed seismic trace a) using a Morlet wavelet, b) using a Gaussian wavelet and c) using a Mexican hat wavelet. Note how the Mexican hat option yields a clear spectral response with higher vertical resolution than does the Morlet wavelet and a higher lateral resolution than the Gaussian wavelet.

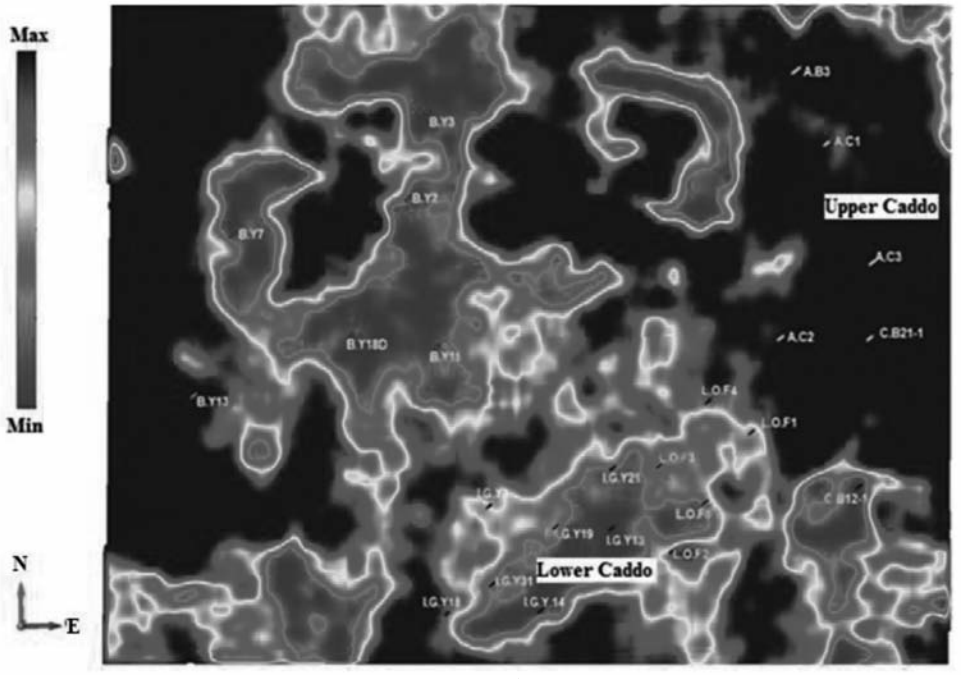

Fig. 9. 50-Hz horizon shows Lower and Upper Caddo reservoirs distributions. Note that all Lower Caddo producing wells (in black) are associated with low amplitude, while Upper Caddo producing wells (in white) are associated with high amplitude.

We propose the following interpretation for these amplitude changes. The high-amplitude anomaly shown in the zone encompassing Upper Caddo wells can be attributed to the following fact. In the presence of hydrocarbons, encasing formations selectively reflect some particular frequencies and do not reflect others. Thus, at 50-Hz in particularly the Upper Caddo reservoir is significantly brighter than other adjacent formations. One can attribute this high amplitude to a thin-bed effect and hydrocarbon charge. The hydrocarbon presence makes the reservoir reflection coefficients larger than those of other surrounding areas, and the thin-bed tuning effects preferentially reflect a 50-Hz signal making the 50-Hz image brighter than other frequencies.

Contrary, in the Lower Caddo reservoir we have noticed very low amplitude spectral responses at this frequency (50-Hz) relative to that was seen in elsewhere. Note that the anomalously low-frequency trend is found to match the Lower Caddo reservoir distribution and geographic bounds implied by well control (Fig. 10). This frequency response is assumed to be associated with high

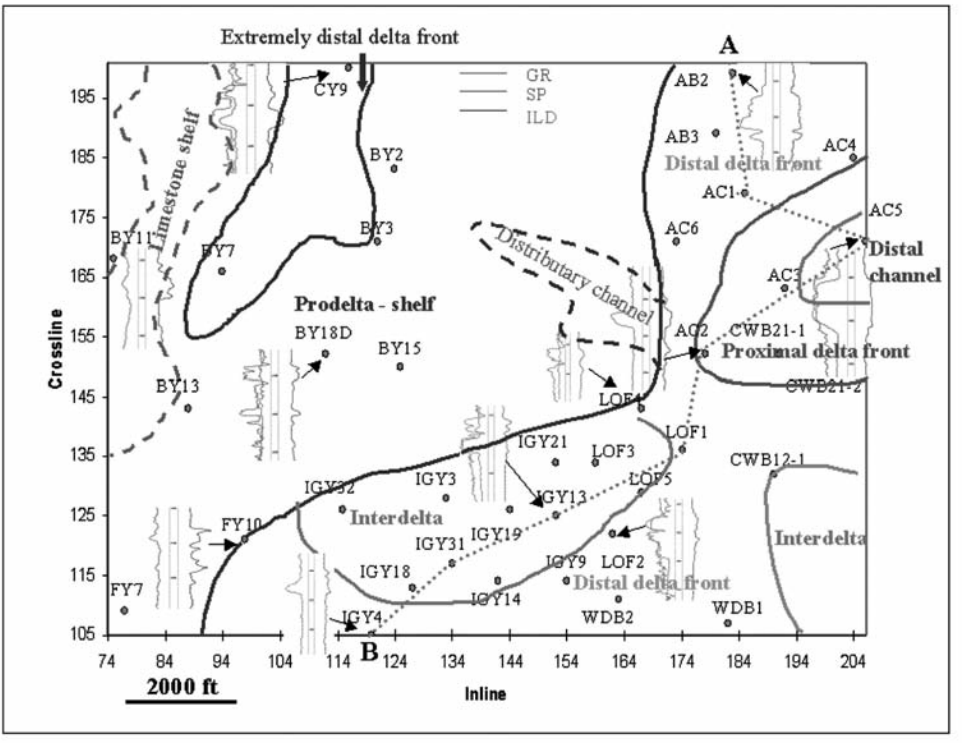

Fig. 10. Representative well log trends and depositional sub-facies of the Caddo sequence based on well data (From Xie et al., 2004).

attenuation of high frequencies have encountered while traveling through hydrocarbon bearing reservoirs. Notice that although reservoirs are so close, their frequency responses are very different. This difference can be partly associated with their thicknesses, as thickness is one of the key factors controlling reservoir's spectral decomposition responses. Note that both observed frequency behaviors are well illustrated in Castagna et al. (2003) and Burnet et al. (2003).

It is important also to point out that there are other areas where neither Lower Caddo nor Upper Caddo reservoirs were penetrated that show somewhat similar frequency responses to those discussed above. That is, the low amplitude spectrum anomaly passing through the wells B.Y2, B.Y3 and B.Y18D is similar to that of the Lower Caddo. Thus, anomalously low amplitude spectrum is not a reliable diagnostic of a hydrocarbon-charged Caddo formation. We have selected several individual traces at producing well locations and traces at

non-producing wells zones for more detailed spectral analysis and calibration. Figs. 11 and 12 depict spectrum decomposition of single traces from Lower Caddo producing wells (I.G.Y13, 21 and 31) and traces from wells positioned in the limestone zone (B.Y3,18D and 15), respectively.

Note that information in individual traces comes from consistently gridded small zones (110 ft x 110 ft). Frequency images from these traces revealed that frequency behaviors of hydrocarbon-producing zones and limestone-dominated zones are different although they appear similar in the frequency response map. That is, Lower Caddo trace examination shows that high frequencies are present but undergo severe attenuation exactly at the reservoir depth location (Fig. 11).

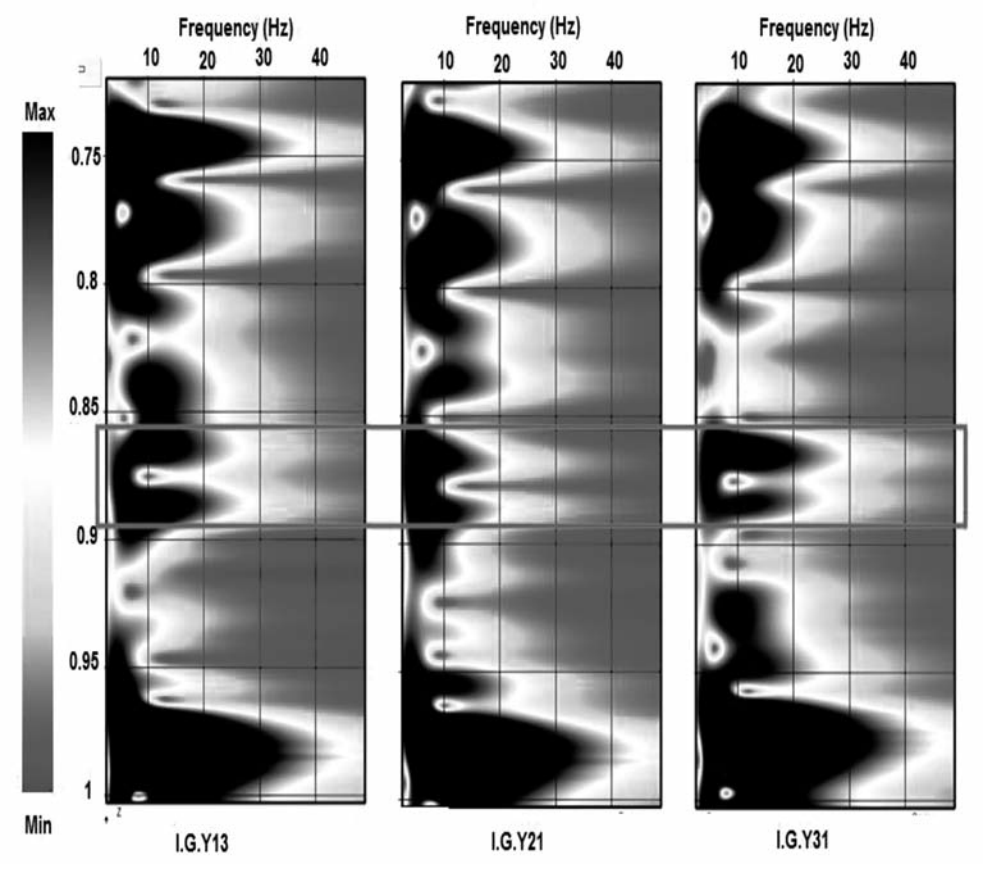

Fig. 11. Frequency response at the lower Caddo reservoir followed by low frequency immediately below the reservoir interval observed in the three wells: I.G.Y13 (left), I.G.Y21 (middle) and I.G.Y31 (right).

The attenuated frequencies are followed by a low frequency character immediately below the reservoir interval. On the other hand, in the traces from the non-producing zone, these high frequencies are almost absent and are followed by a high-frequencies character, immediately below the reservoir interval (Fig. 12). The low frequency presence, in Fig. 11, is commonly associated with hydrocarbon reservoirs where the thickness is not sufficient to result in significant attenuation (Castagna et al., 2003; Castagna and Sun, 2006).

Thus, the spectral decomposition provides information that separates non-producing limestone beds from hydrocarbon encasing formations.

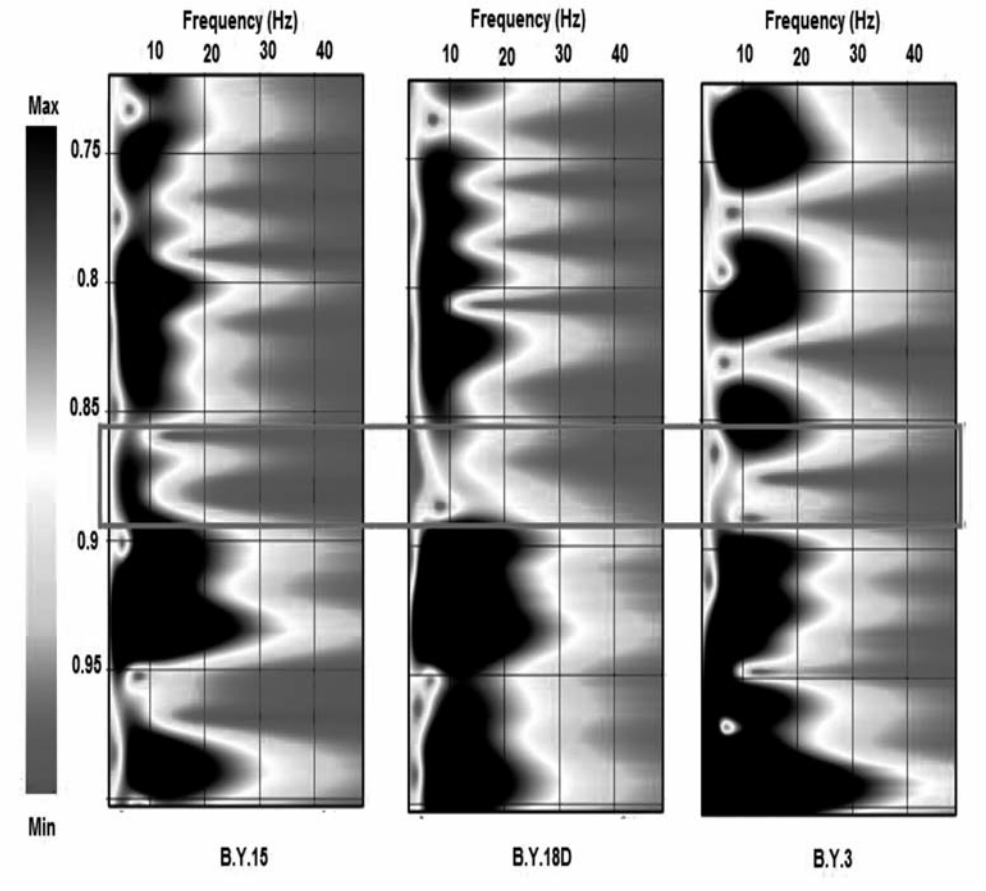

Fig. 12. Non-producing formation frequency response at three well locations observed in the three wells: B.Y.15 (left), B.Y.18D (middle) and B.Y.3 (right). Note that the high-frequency responses observed previously in Fig. 10 are almost absent at the reservoir interval (highlighted). A high frequency increase is observed immediately below the zone of study.

Finally, in order to provide more support to our interpretation, seismic inversion has been carried out to create an acoustic impedance volume from the integration of well data and seismic. Note that an acoustic impedance cube has several advantages over conventional seismic data. Contrary to seismic data that deliver layer boundary properties, an inversion volume provides the geoscientist with a rock property that is directly related to lithology, porosity, and fluid content. In this regard, four wells have been correlated to a small seismic cube to produce an acoustic impedance volume. An excellent match between synthetic and real data was reached with minimum misfit error.

As expected, the acoustic inversion sections could go beyond the seismic data and infer more key information. The impedance sections in Figs. 13 and 14 demonstrate that producing wells used for the detailed spectral analysis in Figs. 11 and 12 penetrate the Upper Caddo reservoir characterized by high impedance. In contrast, dry well B.Y.18D appears with relatively low impedance, as Fig. 14 displays. Note that the incised valley-fill reservoirs in our

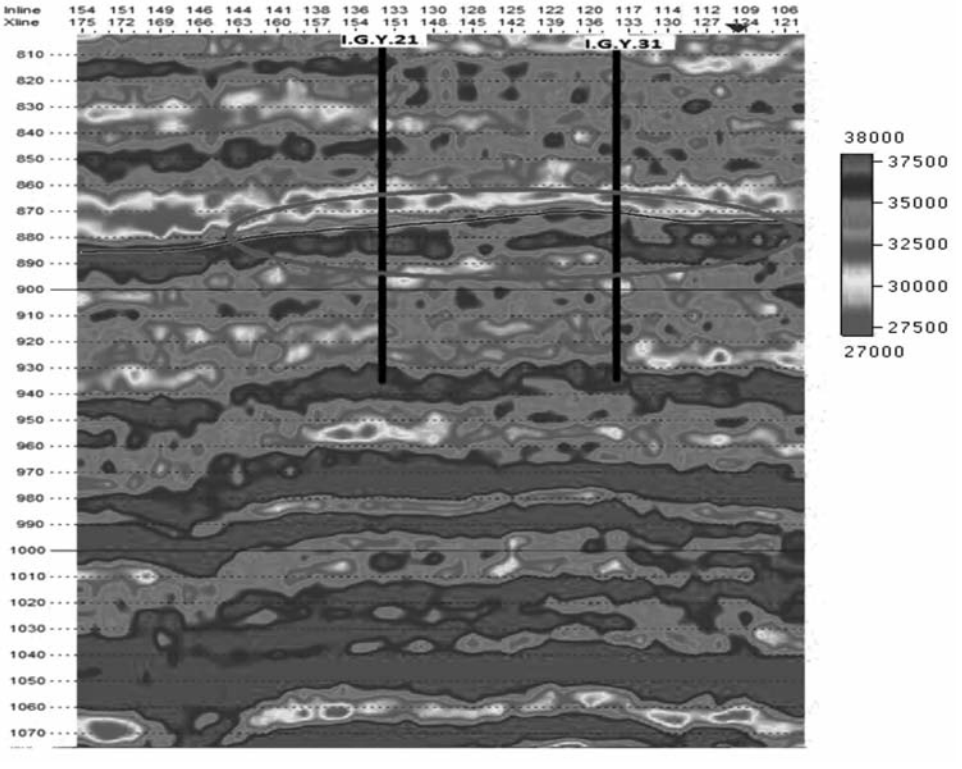

Fig. 13. Acoustic impedance section demonstrates that producing wells (I.G.Y31 and I.G.Y21) penetrate Upper Caddo reservoirs characterized by high impedance.

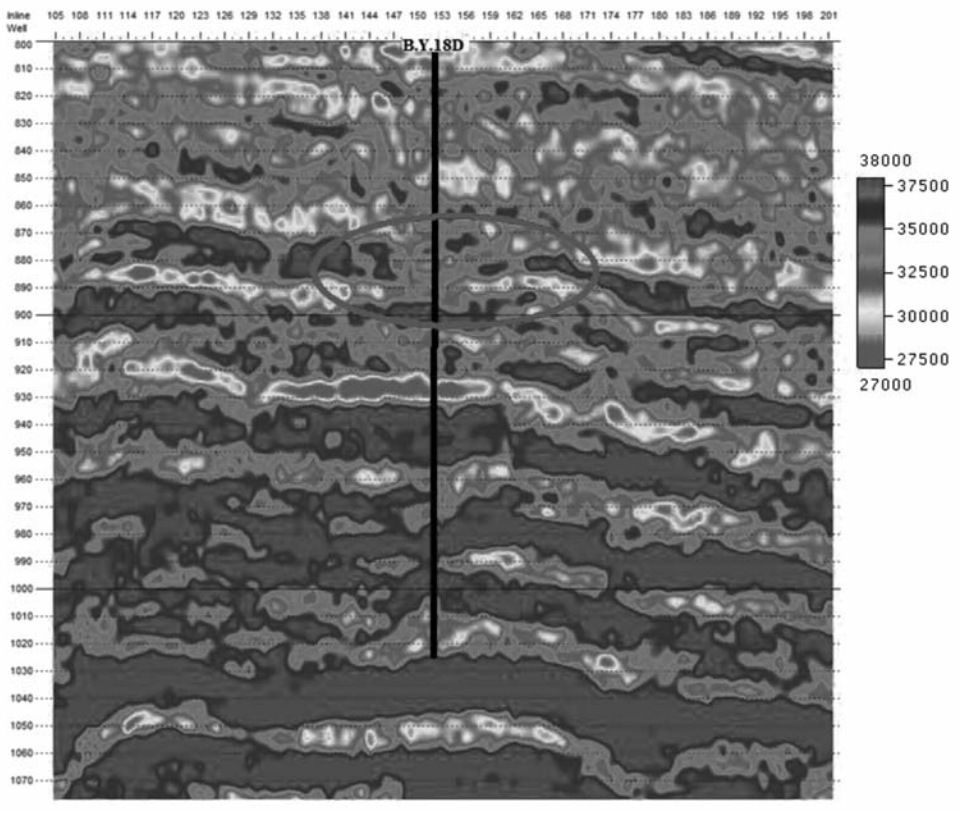

Fig. 14. Acoustic impedance section demonstrates that dry well B.Y.18D appears with relatively low impedance and do not pass through the Upper Caddo reservoir characterized by high impedance.

area exhibit relatively higher density and velocity compared to their surrounding rocks. It is clear that the impedance character associated with Caddo reservoirs do not reach the well B.Y.18D or cross it. At wells I.G.Y31 and IGY21, the high Caddo reservoir impedance character passes through both wells. This attribute behavior not only supports the spectral decomposition results but removes remaining ambiguity in achieving our objective.

CONCLUSION

Seismic data and conventional seismic attributes are ambiguous in differentiating targeted Caddo reservoirs. However, the successful integration of different modern approaches (steered filtering, dense tracking, spectral

decomposition and seismic inversion) revealed stratigraphic information of the two reservoirs separated by thin bed limestone. The advanced filtering and tracking techniques allowed us to produce clean attribute maps with higher resolution and improved interpretability. Spectral decomposition images helped identify our targeted reservoirs distributions. Acoustic impedance inversion provided more information about reservoirs properties and supported spectral decomposition interpretation.

REFERENCES

Burnett, M.D., Castagna, J.P., Méndez-Hernández, E., Rodríguez, G.Z., García, L.F., Martínez-Vázquez, J.T., Avilés, M.T. and Vila-Villaseñor, R., 2003. Application of spectral decomposition to gas basins in Mexico. The Leading Edge, 22: 1130-1141.

Burns, S. and Street, K., 2005. Spectral decomposition highlights faults. Hart's E&P, March, http://www.epmag.com/archives/digitalOilField/2135.htm.

Castagna, J.P., Sun, S. and Siegfried, R.W., 2003. Instantaneous spectral analysis: Detection of low-frequency shadows associated with hydrocarbons. The Leading Edge, 22: 120-127.

Castagna, J. and Sun, S., 2006. Comparison of spectral decomposition methods. First Break, 24: 75-79.

Chopra, S. and Marfurt, K.J., 2007. Seismic Attributes for Prospect Identification and Reservoir Characterization. SEG, Tulsa, OK, 456 pp.

De Grout, P., Huck, A., de Bruin, G., Hemstra, N. and Bedford, J., 2010. The horizon Cube: A step change in seismic interpretation. The Leading Edge, 29: 1048-1055.

Farfour, M., Yoon, W.J., Jo, Y. and Kim, Y.W., 2013. Spectral decomposition and reservoir engineering data in mapping thin bed reservoir, Stratton Field, South Texas. J. Seismic Explor., 22: 77-91.

Hampson, D., Russell, B. and Bankhead, B., 2005. Simultaneous inversion of pre-stack seismic data. Expanded Abstr., 75th Ann. Internat. SEG Mtg., Houston.

Hardage, B.A., Carr, D.L., Lancaster, D.E., Simmons, J.L., Hamilton, D.S., Elphick, R.Y., Oliver, K.L. and Johns, R.A., 1996a. 3D seismic imaging and seismic attribute analysis of genetic sequences deposited in low accommodation conditions. Geophysics, 61: 1351-1362.

Hardage, B.A., Simmons, J.L., Lancaster, D.E., Elphick, R.Y., Edson, R.D., and Carr, D.L., 1996b. Boonsville 3-D Seismic Data Set. The University of Texas at Austin, Bureau of Economic Geology, 32 pp.

Mallat, S., 2008. A Wavelet Tour of Signal Processing. Academic Press Inc., New York.

Partyka, G., Gridley, J. and Lopez, J.A., 1999. Interpretational applications of spectral decomposition in reservoir characterization. The Leading Edge, 18: 353-360.

Roksandic, M.M., 1995. On: "3-D seismic imaging and seismic attribute analysis of genetic sequences deposited in low- accommodation conditions" (B.A. Hardage, D.L. Carr, D.E. Lancaster, J.L. Simmons Jr., D.S. Hamilton, R.Y., Elphick, K.L., Oliver and R.A. Johns, Geophysics, 61: 1351-1362). Geophysics, 60: 1585-1587.

Tanakov, M.Y. and Kelkar, M., 2000. Integrated Reservoir Description for Boonsville, Texas Field Using 3D Seismic Well and Production Data. Society of Petroleum Engineering, SPE 59693.

Xie, D., Wood, J.R. and Pennington, W.D., 2004. Quantitative seismic facies analysis for thin-bed reservoirs: A case study of the central Boonsville Field, Fort Worth Basin, North-central Texas. Expanded Abstr., 74th Ann. Internat. SEG Mtg., Denver: 1484-1487.

Yoon, W.J. and Farfour, M., 2012. Spectral decomposition aids AVO analysis in reservoir characterization: A case study of Blackfoot field, Alberta, Canada. J. Comput. Geosci., 46: 60-65.